

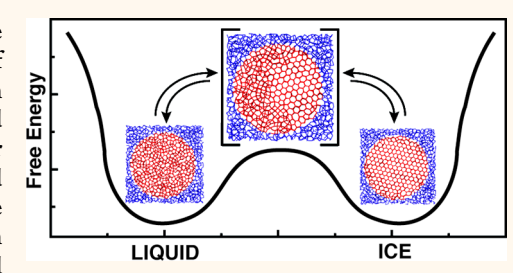
## Ice-Liquid Oscillations in Nanoconfined Water

Noah Kastelowitz and Valeria Molinero\*

Department of Chemistry, The University of Utah, 315 South 1400 East, Salt Lake City, Utah 84112-0850, United States

Supporting Information

ABSTRACT: Nanoscale confinement has a strong effect on the phase behavior of water. Studies in the last two decades have revealed a wealth of novel crystalline and quasicrystalline structures for water confined in nanoslits. Less is known, however, about the nature of ice-liquid coexistence in extremely nanoconfined systems. Here, we use molecular simulations to investigate the ice-liquid equilibrium for water confined between two nanoscopic disks. We find that the nature of ice-liquid phase coexistence in nanoconfined water is different from coexistence in both bulk water and extended nanoslits. In highly nanoconfined systems, liquid water and ice do not coexist in space because the two-phase states are



unstable. The confined ice and liquid phases coexist in time, through oscillations between all-liquid and all-crystalline states. The avoidance of spatial coexistence of ice and liquid originates on the non-negligible cost of the interface between confined ice and liquid in a small system. It is the result of the small number of water molecules between the plates and has no analogue in bulk water.

KEYWORDS: phase transitions, confinement, water, crystallization, bilayer ice, dynamics, nucleation

lassical and ab initio molecular simulation studies have revealed a wealth of crystalline and quasicrystalline structures for water confined between parallel walls, 1-8 several of which were later identified in experiments.<sup>9,10</sup> Bilayer hexagonal (BH) ice is the stable crystal of a water bilayer at low pressures and consists of two layers of flat hexagons stacked in registry.3 Among the many crystals formed in slit confinement, BH is noteworthy for its anomalously high melting temperature, 11 which simulations with the mW, TIP4P/Ice, TIP4P, and SPC/E models have been determined to be above the melting temperature for bulk hexagonal ice and quite insensitive to the hydrophobicity or hydrophilicity of the confining plates.<sup>3,4,11-13</sup> This indicates that confined bilayer hexagonal ice is stable at temperatures for which bulk water is a stable liquid.

Past studies of crystallization of water confined in nanoslits have focused on confinement by macroscopic plates. Water in biology and in materials, however, can be confined by surfaces that are themselves nanoscopic. This can have momentous implications for the nature of phase coexistence. The free energy of a two-phase (e.g., liquid-ice) system is a linear combination of the free energies of each phase and the free energy of their interfaces. Although interfaces decrease the stability of the two-phase system, they represent a negligible contribution to the total free energy of extensive systems, allowing for spatial coexistence of two phases in any proportion at the equilibrium temperature. This is not the case for systems with a small number of molecules, for which the cost of the interface destabilizes configurations containing two phases. The result is phase coexistence that is qualitatively different from the one observed in bulk systems, with equilibrium achieved through temporal oscillations between the two phases. 14-16 Liquid-vapor oscillations observed in simulations of water confined between nanoscopic hydrophobic surfaces<sup>17-27</sup> and liquid-crystal oscillations in small clusters<sup>28-30</sup> are examples of this rare behavior.

To our knowledge, liquid-crystal oscillations have not yet been conclusively identified in experiments. Their experimental study has been hampered by the metastability of both phases with respect to vapor in clusters, the difficulty to control simultaneously the thermodynamic state and size of the clusters, and the convergence of the melting and glass transitions in small aggregates.<sup>31</sup> Here, we use molecular simulations to study stable ice-liquid transitions in confined water systems that allow for size and thermodynamic control and present oscillations at temperatures well above the glass transition

We investigate the equilibrium between ice and liquid in water bilayers confined by nanoscopic disks and open to a bath of liquid water. This type of nanoscopic confinement could occur in natural and synthetic materials and also in biological systems. We demonstrate that the nanoconfined water bilayers display ice-liquid coexistence through oscillations between allice and all-liquid states. We characterize the thermodynamics and kinetics of these transitions and show that the quasi-twodimensional (2D) confinement by the disks results in iceliquid oscillations in bilayers with diameters as large as 7 nm to our knowledge, the largest ever reported for heterophasic

Received: May 5, 2018 Accepted: July 19, 2018 Published: July 19, 2018

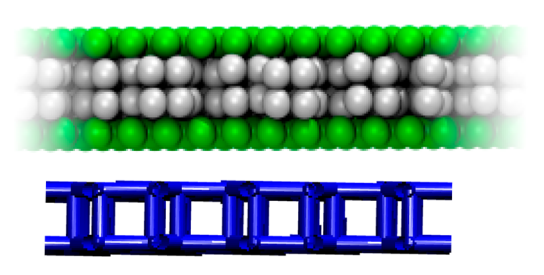


oscillations—at temperatures *above* the melting temperature of bulk ice.

## **RESULTS AND DISCUSSION**

We perform molecular simulations with the mW water model<sup>32</sup> to investigate the nature of the liquid—ice equilibrium of water confined between nanoscopic plates. We characterize the equilibrium between bilayer liquid water and BH ice confined between two identical nanoscopic disks of diameter D=7.2, 4.3, 2.9, and 1.7 nm. The separation between the two disks, 0.85 nm, accommodates two layers of water molecules (Figure 1). The water confined between the disks is open to a bath of

# a) Confined bilayer hexagonal ice exposes squares in its rim to the liquid



b) Confined ice I exposes hexagons

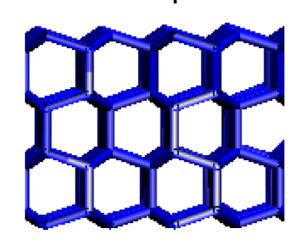


Figure 1. Bilayer hexagonal (BH) ice has a structure distinct from that of ice I. (a) The two layers of water in BH are in registry and tiled with flat hexagons. The top panel shows a side view of the bilayer (white balls) and the confining plates (green balls); the lower panel shows the water—water bonding (blue sticks) for a detail of the same view. (b) Water—water bonds in detail of four-layer ice, which has the structure of ice I, confined between the same plates. BH exposes only square rings to liquid water, whereas confined ice I exposes hexagonal rings. The ice—liquid equilibrium temperature of confined ice I is always lower than that for bulk water. 11,34

liquid water at 1 bar and temperature T, with which it freely exchanges molecules. The melting temperature of the extended ice bilayer is 280 K,<sup>11</sup> higher than the 273 K melting point of ice  $I_h$  in the mW model.<sup>33</sup>

Figure 2a presents the time evolution of the number of molecules in the ice phase for water contained between open plates with 7.2 nm diameter at 278.75 K. Water between the plates oscillates between all-liquid and all-ice states (Figure 2a,b and Supporting Movie S1). The range of temperatures  $\delta T$  for which there is at least 1% of each phase in the oscillating system can be predicted from its equivalence temperature  $T_{\rm eq}$  (at which the free energy of the confined liquid and ice phases are the same) and the change in free energy gap between the two phases with temperature, that is, the entropy of melting of the bilayer  $\Delta S_{\rm m} = 11.4$  J K<sup>-1</sup> mol<sup>-1</sup>,  $^{11}$  as  $\delta T = \ln(100)RT_{\rm eq}/(N\Delta S_{\rm m})$ ,  $^{15,16}$  where R is the gas constant,  $T_{\rm eq} = 278.5$  K (Figure 2c), and  $N \approx 800$  is the number of water molecules

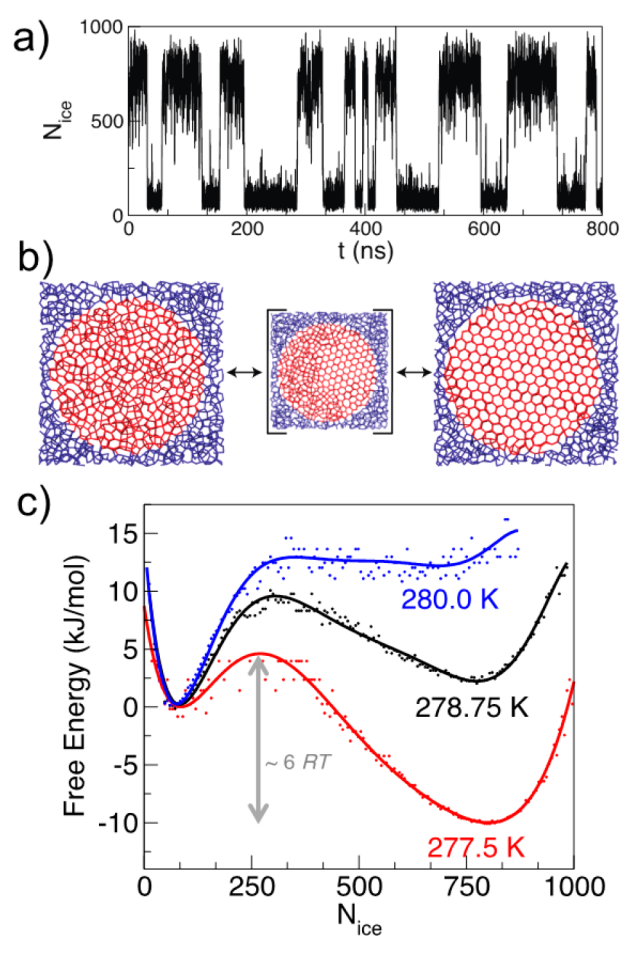


Figure 2. Ice—liquid phase coexistence through oscillations in water confined between 7.2 nm diameter plates open to a bath of liquid water at 1 bar and the temperature indicated. Top panel: number of confined water molecules in the ice phase as a function of time at 278.75 K. Middle panel: liquid (left), unstable ice plus liquid intermediate (middle), and ice (right) phases of nanoconfined water (red) coexist in equilibrium with bulk liquid water (blue). For clarity, only the water molecules in the 0.85 nm slice of the system corresponding to the width of the confined system is shown. Supporting Movie S1 displays the full 800 ns simulation trajectory at 278.75 K. Bottom panel: free energy profile along the crystallization coordinate defined by the number of molecules in the confined ice phase, computed from the probabilities  $P(N_{\rm ice})$  along 800 ns long simulation trajectories; the points represent  $\Delta G = -RT \ln P(N_{\rm ice})$  and the lines their smooth interpolation.

between the plates (Figure 2). This predicts a range of  $\delta T=1.3$  K for which each phase will be observed at least 1% of the time, in good agreement with the results of Figure 2. The relatively small value of the entropy of melting of bilayer ice (about 60% of the bulk value 32) contributes to the existence of a sizable range of temperatures  $\delta T$  for which ice—liquid oscillations are significant, even for the largest disks. We note that  $\Delta S_{\rm m}$  is very robust across water models, such as mW, TIP4P, and TIP4P/Ice. 411,32 The melting temperature of the bilayer can be modulated by the interactions between the water and the confining walls and can reach values much higher than  $T_{\rm m}^{\rm bulk}$  (e.g.,  $T_{\rm m}^{\rm bilayer}=317$  K for a TIP4P/ice water confined between plates that interact with water through a Lennard-Jones 9-3 potential with  $\varepsilon=2$  kJ mol $^{-1}$ ). Hence, we expect that oscillations between all-ice and all-liquid states of bilayer

water will also occur in nanoconfined water in experiments at temperatures above 0  $^{\circ}$ C.

The range of temperatures for which confined ice and liquid coexist through oscillations depends on the size of the confining disks (Figure 2c and Supporting Figure S1), as predicted by the inverse dependence of  $\delta T$  with the number of water N between the plates. This range narrows as the plates widen, converging to the macroscopic behavior of a single coexistence temperature for large plates. Figure 3 summarizes

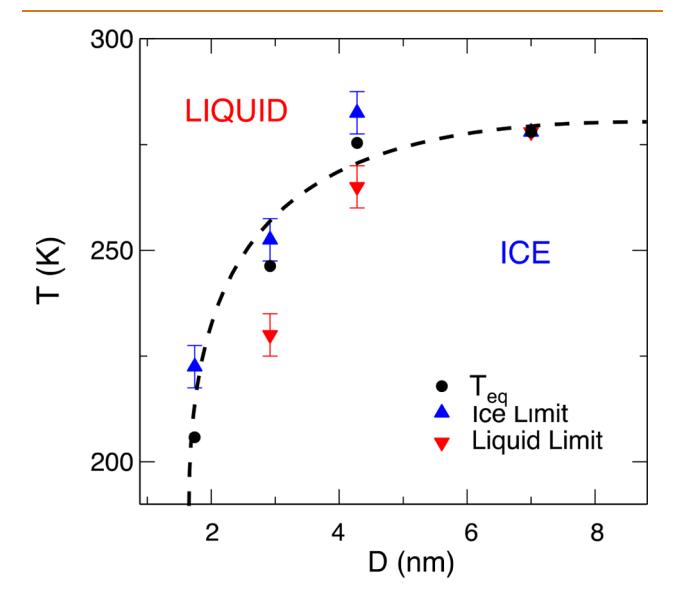


Figure 3. Phase diagram of bilayer water confined between plates of diameter D open to bulk liquid water at temperature T and 1 bar. The black circles indicate the equivalence temperature  $T_{\rm eq}$ , at which the two confined phases have the same free energy. The blue and red triangles indicate the temperatures for which the confined ice and liquid, respectively, become unstable. Between these two boundaries, confined water oscillates between ice and liquid states. The limit of stability of the liquid cannot be determined for the smallest plate because it occurs at a temperature below the homogeneous nucleation of mW ice, 202 K. The dashed line is a guide for the eyes. Water confined by the D=7.2 nm disks oscillates within has a temperature rangesmaller than 2 K, and its equilibrium temperature is almost indistinguishable from the temperature of equilibrium of the infinite bilayer.

the limits of stability of ice and liquid, that is, the temperatures for which the free energy curves lose the corresponding minimum and the equivalence temperatures as a function of disk diameter. Confined liquid and ice become thermodynamically unstable at temperatures below or above, respectively, the ice—liquid coexistence range. In contrast, there is no known thermodynamic limit of stability (*i.e.*, spinodals) for crystal—liquid transitions in the extended bilayer or in bulk systems.

The barrier that separates ice and liquid at the equivalence temperature is finite and comparable to the thermal energy. This allows for fast transitions between ice and liquid states. In contrast, homogeneous nucleation of a new phase in a macroscopic system cannot occur at the equilibrium temperature because the size of the critical nucleus and the free energy barrier diverge in the absence of a thermodynamic driving force. We note that structural fluctuations in the confined system are not necessarily larger than that in the extended bilayer: relatively small fluctuations suffice to turn the whole confined water to the other phase. We conclude that

confined ice and liquid display fast oscillations at the equivalence temperature because the length scales of structural fluctuations at equilibrium are comparable to the dimensions of the whole confined system.

The barrier that controls the heterophasic oscillations occurs when ~40% of the confined water has crystallized, irrespective of the disk size (Figure 2 and Supporting Figure S1). Both bilayer liquid and ice are in contact with the external liquid bath at the top of the barrier (Figure 2b). From the fraction and spatial distribution of ice at the top of the barrier, we infer that the surface tension between the confined bilayer ice and confined liquid with the external liquid bath are comparable, only slightly higher for BH ice than for bilayer liquid. This contrasts with liquid—vapor oscillations in confinement, in which the large value of liquid—vapor surface tension leads to tubular (or hourglass) bubbles. <sup>17,18,24,25,36</sup>

The height of the barrier for the ice-liquid oscillations decreases with the diameter of the disk because the smaller the disk, the lower the number of water molecules at the interface between the two confined phases in the transition state. If we neglect the difference in free energy cost of the interface between the bulk liquid/bilayer ice and bulk liquid/bilayer liquid and treat the bilayer water as a quasi-2D system, then the barrier between the all-ice and all-liquid state at  $T_{\rm eq}$  is given by  $\tau l$ , where  $\tau$  is the line tension of the bilayer liquid—ice interface and its length *l*. We determine  $\tau \approx 2$  pN from the barriers at the equivalence points assuming l = D (Figure 2b). For comparison,  $\tau$  between BH ice and bilayer liquid is two times larger than the one between cubic and hexagonal ice, and when normalized by the height  $h \approx 0.4$  nm, the bilayer results in an ice-liquid surface tension within the bilayer,  $\gamma_{\rm bilayer} = \tau/h \approx 5$  mJ m<sup>-2</sup>, that is much smaller than the bulk ice—liquid surface tension,  $\gamma_{\text{bulk}}$  = 35 mJ m<sup>-2 37,38</sup> The unusually low cost of the bilayer liquid-BH ice interface, together with the quasi-2D geometry of the confinement, makes the barrier between the two phases comparable to the thermal energy.

The smaller the plates, the lower the barrier between the liquid and ice states, increasing the likelihood that a thermal fluctuation will trigger the phase transition. This results in shorter lifetimes of each nanophase, that is faster ice—liquid oscillations, for water confined between the smaller plates, as seen in Figure 4. We find that the lifetime of each phase at the corresponding equivalence temperature scales with the plate diameter as  $ln(\tau/ns) \approx 0.85 \text{ nm}^{-1} (D-1.64 \text{ nm})$ . The exponential scaling of the lifetime with D is consistent with a transition barrier controlled by  $\tau D$ . We find that liquid and ice states are ill-defined for plates with a diameter smaller than 1.7 nm. As the mW model reproduces the thermodynamics of water but overestimates its diffusion coefficient (by 4.5 times at 273 K<sup>32</sup>), we expect that the transition times will be longer for nanoconfined water in experiments.

The number of molecules involved in the phase oscillations of the confined bilayer, over 800, is significantly larger than the up to ~130 molecules involved in ice—liquid oscillations in water clusters. <sup>29,30,39-41</sup> We note that oscillatory behavior has been mostly reported for clusters with less than 20 molecules and should be considered isomerizations rather than phase transitions. Oscillations between ice I and liquid have only been reported for clusters with 137 molecules (1 nm radius), most of which are at the disordered surface, leaving a tiny core that alternates between ice and liquid states. <sup>29</sup> The distinctly higher size of systems for which ice—liquid oscillations occur in

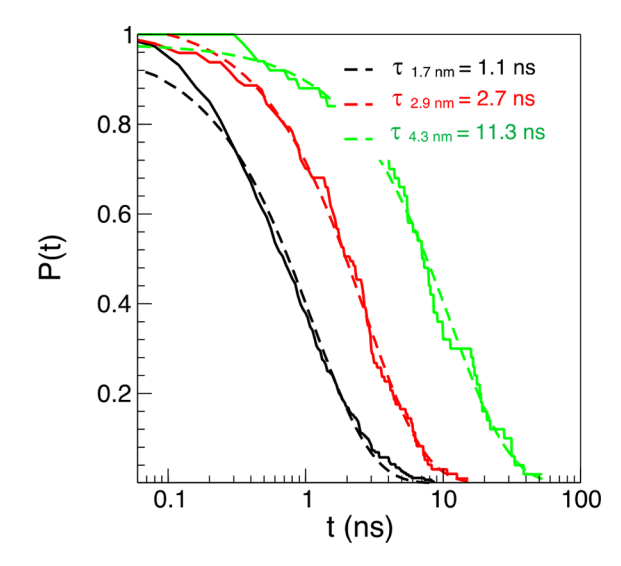


Figure 4. Distribution of survival times of each nanophase of the water bilayer confined by disks of diameter D=1.7 nm (black solid line), D=2.9 nm (red solid line), and D=4.3 nm (green solid line) at the corresponding equivalence temperatures , collected over 800 ns long simulations. The dashed lines correspond to exponential fits to these data, with characteristic times indicated in the labels. The 800 ns simulation of water confined in the D=7.2 diameter disks (Figure 2a) is insufficient to build the corresponding histogram but renders an average lifetime of  $\sim$ 50 ns at its equivalence temperature.

bilayer water is due to the lower fraction of molecules in the ice-liquid interface in disk versus sphere geometries and the very low cost of the BH-bilayer liquid interface. Moreover, whereas clusters are metastable with respect to evaporation, bilayer water confined between two nanoscopic plates is a thermodynamically stable system in equilibrium with liquid water. We find that even when the bilayer oscillates below the melting point of bulk water, the exposure of the rim of the ice bilayer is insufficient to trigger the heterogeneous nucleation of ice in the bath. This inability of BH ice to heterogeneously nucleate ice I even at temperatures close to the homogeneous nucleation temperature of mW water, 202 K (Figure 3), is probably due to the unique structure of BH ice, which exposes a rim of water squares to the bath. 11 These results suggest that ice-liquid oscillations could exist in confined water exposed to both stable and supercooled water. The existence of these oscillations could have important implications for the control of solute transport and may be used to design valves that have different fraction of open and closed times as a function of temperature. Crystal-liquid oscillations on other systems, for example, the structurally analogous silicon bilayers, 42 could result in transitions between metallic and semiconducting

The coexistence of confined ice and liquid through temporal oscillations originates on the same small-system physics that produces liquid—vapor oscillations. The latter, however, necessitates confinement of water by highly hydrophobic surfaces to destabilize the liquid phase.<sup>24</sup> The equilibrium between BH ice and bilayer liquid, on the other hand, occurs above the melting point of bulk ice for both hydrophobic and hydrophilic confinement.<sup>3,4,11-13</sup> As the cost of the ice—liquid interface for bilayer water is less than 10% of the cost of the liquid—vapor interface, the time scales of the oscillations between confined ice and liquid are several orders of

magnitude faster<sup>17,18</sup> than that between liquid and vapor confined between plates of comparable sizes. Flexibility of the confining surfaces has been found to have an important effect on wetting—drying transitions<sup>43</sup> and in the equilibrium between water multilayers.<sup>44</sup> It would be interesting to explore in future studies the role of flexibility on the ice—liquid transitions of nanoconfined water.

## **CONCLUSIONS**

We use molecular simulations to demonstrate that a water bilayer confined between disks of nanoscopic dimensions can display heterophasic crystal-liquid oscillations at temperatures that reach above the melting point of bulk water. These oscillations are a consequence of the small number of confined molecules, which penalizes spatial coexistence because the fraction of molecules at the interface between confined liquid and crystal is not negligible, but still results in a barrier small enough to be crossed through thermal fluctuations. There is no analogous behavior in bulk water (e.g., a glass of water oscillating between all-ice and all-liquid states at 0 °C) because the barrier that separates the macroscopic all-ice and all-liquid states at the melting point scales with the number of molecules at the interface and cannot be overcome with thermal fluctuations in a macroscopic system. Extreme confinement changes not only the structure and stability of water phases but also the nature of their phase coexistence.

#### **METHODS**

We perform molecular dynamics simulations using LAMMPS.<sup>45</sup> Water is represented with the mW model, which has been extensively used to investigate the crystallization of bulk and confined water. 4,5,11,29,34,35,46-59 The plates are circular cutoffs with diameters of 7.2, 4.3, 2.9, and 1.7 nm from a triangular lattice with interparticle distance of 0.32 nm. A triangular lattice was selected because it cannot template ice order; hence, it ensures that the formation of BH is not biased by the structure of the confining surfaces.  $^{11}$  We have shown in ref 11 that BH also forms and is stable above the melting point of ice I when confined by featureless Lennard-Jones 9-3 plates, and that the stability of BH is quite insensitive to the strength of the water-plate interaction, that is, the hydrophilicity of the confining plates. The number of particles in the plates ranges from 433 to 7 particles. Each simulation cell is periodic in the three dimensions and contains two parallel disks of a given size positioned 0.85 nm apart and with water-up to 11 250 molecules in the simulations with the largest disks—surrounding the disks and in the space between them. The separation between the disks is selected to maximize the melting temperature of bilayer ice.<sup>11</sup> Water and the particles in the plates interact through a two-body Stillinger-Weber potential with strength  $\varepsilon = 1.7 \text{ kJ mol}^{-1}$  and  $\sigma = 3.56 \text{ Å}.^{11}$  Interaction between the particles in the plates are not considered because the plates are rigid. The equations of motion of water are integrated with the velocity Verlet algorithm using a time step of 10 fs. The temperature and pressure are controlled with the Nose-Hoover thermostat and barostat with damping times of 5 and 25 ps, respectively. The systems are first equilibrated for 10 ns, after which we perform simulations for up to 800 ns and collect the configurations for analysis. The number of molecules in BH ice,  $N_{\rm ice}$ , is determined as in ref 11. The free energy profiles are computed from the histogram  $P(N_{ice})$ ,  $\Delta G = -RT \ln$  $P(N_{ice})$ , and reported with the zero set for the minimum of the liquid state. The equivalence  $T_{\rm eq}$  is determined as that for which the depth of the free energy minima of confined liquid and ice are the same; the limit of stability of the confined liquid and phases is identified as that for which the corresponding minimum disappears from the free energy profiles. The lifetimes of each phase are computed from the simulation trajectories closest to the equivalence temperature of each

system, by first computing a histogram of survival time of each phase and then fitting that histogram to exponential decays.

## **ASSOCIATED CONTENT**

## **S** Supporting Information

The Supporting Information is available free of charge on the ACS Publications website at DOI: 10.1021/acsnano.8b03403.

Supporting figure with the free energy profiles for smaller disks and the movie caption (PDF)

Movie file that shows the oscillations in the largest disk at the equivalence temperature (AVI)

## **AUTHOR INFORMATION**

## **Corresponding Author**

\*E-mail: valeria.molinero@utah.edu.

ORCID ®

Valeria Molinero: 0000-0002-8577-4675

Notes

The authors declare no competing financial interest.

## **ACKNOWLEDGMENTS**

We gratefully acknowledge support by the Beckman Foundation through a Young Investigator Award, the National Science Foundation through award CHE-1305427, and the Center for High Performance Computing at The University of Utah.

## **REFERENCES**

- (1) Koga, K.; Gao, G. T.; Tanaka, H.; Zeng, X. C. Formation of Ordered Ice Nanotubes inside Carbon Nanotubes. *Nature* **2001**, *412*, 802–805.
- (2) Koga, K.; Zeng, X.; Tanaka, H. Freezing of Confined Water: A Bilayer Ice Phase in Hydrophobic Nanopores. *Phys. Rev. Lett.* **1997**, 79, 5262–5265.
- (3) Koga, K.; Tanaka, H. Phase Diagram of Water between Hydrophobic Surfaces. J. Chem. Phys. 2005, 122, 104711.
- (4) Johnston, J. C.; Kastelowitz, N.; Molinero, V. Liquid to Quasicrystal Transition in Bilayer Water. J. Chem. Phys. 2010, 133, 154516
- (5) Lupi, L.; Kastelowitz, N.; Molinero, V. Vapor Deposition of Water on Graphitic Surfaces: Formation of Amorphous Ice, Bilayer Ice, Ice I, and Liquid Water. *J. Chem. Phys.* **2014**, *141*, 18C508.
- (6) Chen, J.; Schusteritsch, G.; Pickard, C. J.; Salzmann, C. G.; Michaelides, A. Two Dimensional Ice from First Principles: Structures and Phase Transitions. *Phys. Rev. Lett.* **2016**, *116*, 025501.
- (7) Zhu, W.; Zhao, W.-H.; Wang, L.; Yin, D.; Jia, M.; Yang, J.; Zeng, X. C.; Yuan, L.-F. Two-Dimensional Interlocked Pentagonal Bilayer Ice: How Do Water Molecules Form a Hydrogen Bonding Network? *Phys. Chem. Chem. Phys.* **2016**, *18*, 14216–14221.
- (8) Zhao, W.-H.; Wang, L.; Bai, J.; Yuan, L.-F.; Yang, J.; Zeng, X. C. Highly Confined Water: Two-Dimensional Ice, Amorphous Ice, and Clathrate Hydrates. *Acc. Chem. Res.* **2014**, *47*, 2505–2513.
- (9) Kimmel, G. A.; Matthiesen, J.; Baer, M.; Mundy, C. J.; Petrik, N. G.; Smith, R. S.; Dohnálek, Z.; Kay, B. D. No Confinement Needed: Observation of a Metastable Hydrophobic Wetting Two-Layer Ice on Graphene. *J. Am. Chem. Soc.* **2009**, *131*, 12838–12844.
- (10) Algara-Siller, G.; Lehtinen, O.; Wang, F. C.; Nair, R. R.; Kaiser, U.; Wu, H. A.; Geim, A. K.; Grigorieva, I. V. Square Ice in Graphene Nanocapillaries. *Nature* **2015**, *519*, 443–445.
- (11) Kastelowitz, N.; Johnston, J. C.; Molinero, V. The Anomalously High Melting Temperature of Bilayer Ice. J. Chem. Phys. 2010, 132, 124511.
- (12) Lu, Q.; Straub, J. E. Freezing Transitions of Nanoconfined Coarse-Grained Water Show Subtle Dependence on Confining Environment. *J. Phys. Chem. B* **2016**, *120*, 2517–2525.

- (13) Giovambattista, N.; Rossky, P. J.; Debenedetti, P. G. Effect of Pressure on the Phase Behavior and Structure of Water Confined between Nanoscale Hydrophobic and Hydrophilic Plates. *Phys. Rev. E* **2006**, 73, 041604.
- (14) Berry, R. S.; Wales, D. J. Freezing, Melting, Spinodals, and Clusters. *Phys. Rev. Lett.* **1989**, *63*, 1156–1159.
- (15) Berry, R. S.; Smirnov, B. A. Observability of Coexisting Phases of Clusters. *Int. J. Mass Spectrom.* **2009**, 280, 204–208.
- (16) Patashinski, A.; Ratner, M. Heterophasic Oscillations in Nanoscale Systems. *Phys. Rev. E* **2008**, *78*, 041106.
- (17) Xu, L.; Molinero, V. Liquid-Vapor Oscillations of Water Nanoconfined between Hydrophobic Disks: Thermodynamics and Kinetics. *J. Phys. Chem. B* **2010**, *114*, 7320–7328.
- (18) Sharma, S.; Debenedetti, P. G. Evaporation Rate of Water in Hydrophobic Confinement. *Proc. Natl. Acad. Sci. U. S. A.* **2012**, *109*, 4365–4370.
- (19) Remsing, R. C.; Xi, E.; Vembanur, S.; Sharma, S.; Debenedetti, P. G.; Garde, S.; Patel, A. J. Pathways to Dewetting in Hydrophobic Confinement. *Proc. Natl. Acad. Sci. U. S. A.* **2015**, *112*, 8181–8186.
- (20) Sharma, S.; Debenedetti, P. G. Free Energy Barriers to Evaporation of Water in Hydrophobic Confinement. *J. Phys. Chem. B* **2012**, *116*, 13282–13289.
- (21) Cerdeiriña, C. A.; Debenedetti, P. G.; Rossky, P. J.; Giovambattista, N. Evaporation Length Scales of Confined Water and Some Common Organic Liquids. *J. Phys. Chem. Lett.* **2011**, 2, 1000–1003.
- (22) Huang, X.; Margulis, C. J.; Berne, B. J. Dewetting-Induced Collapse of Hydrophobic Particles. *Proc. Natl. Acad. Sci. U. S. A.* **2003**, 100, 11953—11958.
- (23) Luzar, A. Activation Barrier Scaling for the Spontaneous Evaporation of Confined Water. J. Phys. Chem. B 2004, 108, 19859—19866
- (24) Leung, K.; Luzar, A. Dynamics of Capillary Evaporation. II. Free Energy Barriers. *J. Chem. Phys.* **2000**, *113*, 5845.
- (25) Lum, K.; Chandler, D. Phase Diagram and Free Energies of Vapor Films and Tubes for a Confined Fluid. *Int. J. Thermophys.* **1998**, 19, 845–855.
- (26) Beckstein, O.; Sansom, M. Liquid–Vapor Oscillations of Water in Hydrophobic Nanopores. *Proc. Natl. Acad. Sci. U. S. A.* **2003**, *100*, 7063–7068.
- (27) Baron, R.; Molinero, V. Water-Driven Cavity-Ligand Binding: Comparison of Thermodynamic Signatures from Coarse-Grained and Atomic-Level Simulations. *J. Chem. Theory Comput.* **2012**, *8*, 3696–3704
- (28) Kunz, R.; Berry, R. Multiple Phase Coexistence in Finite Systems. *Phys. Rev. E: Stat. Phys., Plasmas, Fluids, Relat. Interdiscip. Top.* **1994**, 49, 1895–1908.
- (29) Johnston, J. C.; Molinero, V. Crystallization, Melting, and Structure of Water Nanoparticles at Atmospherically Relevant Temperatures. *J. Am. Chem. Soc.* **2012**, *134*, 6650–6659.
- (30) Laria, D.; Rodriguez, J.; Dellago, C.; Chandler, D. Dynamical Aspects of Isomerization and Melting Transitions in [H2O]<sub>8</sub>. *J. Phys. Chem. A* **2001**, *105*, 2646–2651.
- (31) Schmidt, M.; von Issendorff, B. Gas-Phase Calorimetry of Protonated Water Clusters. *J. Chem. Phys.* **2012**, *136*, 164307.
- (32) Molinero, V.; Moore, E. B. Water Modeled as an Intermediate Element between Carbon and Silicon. *J. Phys. Chem. B* **2009**, *113*, 4008–4016.
- (33) Hudait, A.; Qiu, S.; Lupi, L.; Molinero, V. Free Energy Contributions and Structural Characterization of Stacking Disordered Ices. *Phys. Chem. Chem. Phys.* **2016**, *18*, 9544–9553.
- (34) Moore, E. B.; Allen, J. T.; Molinero, V. Liquid-Ice Coexistence Below the Melting Temperature for Water Confined in Hydrophilic and Hydrophobic Nanopores. *J. Phys. Chem. C* **2012**, *116*, 7507–7514.
- (35) Moore, E. B.; Molinero, V. Structural Transformation in Supercooled Water Controls the Crystallization Rate of Ice. *Nature* **2011**, *479*, 506–508.

(36) Altabet, Y. E.; Debenedetti, P. G. Communication: Relationship between Local Structure and the Stability of Water in Hydrophobic Confinement. *J. Chem. Phys.* **2017**, *147*, 241102.

- (37) Qiu, Y.; Lupi, L.; Molinero, V. Is Water at the Graphite Interface Vapor-Like or Ice-Like? *J. Phys. Chem. B* **2018**, 122, 3626–3634.
- (38) Espinosa, J. R.; Vega, C.; Sanz, E. Ice—Water Interfacial Free Energy for the TIP4P, TIP4P/2005, TIP4P/Ice, and mW Models as Obtained from the Mold Integration Technique. *J. Phys. Chem. C* **2016**, *120*, 8068–8075.
- (39) Tsai, C. J.; Jordan, K. D. Monte Carlo Simulation of (H2o)8: Evidence for a Low-Energy S4 Structure and Characterization of the Solid ↔ Liquid Transition. *J. Chem. Phys.* **1991**, *95*, 3850–3853.
- (40) Kaneko, T.; Akimoto, T.; Yasuoka, K.; Mitsutake, A.; Zeng, X. C. Size-Dependent Phase Changes in Water Clusters. *J. Chem. Theory Comput.* **2011**, *7*, 3083–3087.
- (41) Egorov, A. V.; Brodskaya, E. N.; Laaksonen, A. Solid-Liquid Phase Transition in Small Water Clusters: A Molecular Dynamics Simulation Study. *Mol. Phys.* **2002**, *100*, 941–951.
- (42) Johnston, J. C.; Phippen, S.; Molinero, V. A Single-Component Silicon Quasicrystal. *J. Phys. Chem. Lett.* **2011**, 2, 384–388.
- (43) Altabet, Y. E.; Haji-Akbari, A.; Debenedetti, P. G. Effect of Material Flexibility on the Thermodynamics and Kinetics of Hydrophobically Induced Evaporation of Water. *Proc. Natl. Acad. Sci. U. S. A.* **2017**, *114*, E2548–E2555.
- (44) Ruiz Pestana, L.; Felberg, L. E.; Head-Gordon, T. Coexistence of Multilayered Phases of Nanoconfined Water: The Importance of Flexible Confining Surfaces. *ACS Nano* **2018**, *12*, 448–454.
- (45) Plimpton, S. Fast Parallel Algorithms for Short-Range Molecular Dynamics. *J. Comput. Phys.* **1995**, *117*, 1–19.
- (46) Moore, E. B.; de la Llave, E.; Welke, K.; Scherlis, D. A.; Molinero, V. Freezing, Melting and Structure of Ice in a Hydrophilic Nanopore. *Phys. Chem. Chem. Phys.* **2010**, *12*, 4124–4134.
- (47) Moore, E. B.; Molinero, V. Growing Correlation Length in Supercooled Water. *J. Chem. Phys.* **2009**, *130*, 244505.
- (48) Moore, E. B.; Molinero, V. Ice Crystallization in Water's "No-Man's Land. J. Chem. Phys. 2010, 132, 244504.
- (49) Moore, E. B.; Molinero, V. Is It Cubic? Ice Crystallization from Deeply Supercooled Water. *Phys. Chem. Chem. Phys.* **2011**, *13*, 20008–20016.
- (50) González Solveyra, E.; De La Llave, E.; Scherlis, D. A.; Molinero, V. Melting and Crystallization of Ice in Partially Filled Nanopores. *J. Phys. Chem. B* **2011**, *115*, 14196–14204.
- (51) Lupi, L.; Hudait, A.; Molinero, V. Heterogeneous Nucleation of Ice on Carbon Surfaces. J. Am. Chem. Soc. 2014, 136, 3156–3164.
- (52) Lupi, L.; Hudait, A.; Peters, B.; Grünwald, M.; Gotchy Mullen, R.; Nguyen, A. H.; Molinero, V. Role of Stacking Disorder in Ice Nucleation. *Nature* **2017**, *551*, 218–222.
- (53) Lupi, L.; Molinero, V. Does Hydrophilicity of Carbon Particles Improve Their Ice Nucleation Ability? *J. Phys. Chem. A* **2014**, *118*, 7330–7337.
- (54) Hudait, A.; Molinero, V. Ice Crystallization in Ultrafine Water-Salt Aerosols: Nucleation, Ice-Solution Equilibrium, and Internal Structure. J. Am. Chem. Soc. 2014, 136, 8081–8093.
- (55) Hudait, A.; Molinero, V. What Determines the Ice Polymorph in Clouds? J. Am. Chem. Soc. 2016, 138, 8958–8967.
- (56) Hudait, A.; Odendahl, N.; Qiu, Y.; Paesani, F.; Molinero, V. Ice-Nucleating and Antifreeze Proteins Recognize Ice through a Diversity of Anchored Clathrate and Ice-Like Motifs. *J. Am. Chem. Soc.* 2018, 140, 4905–4912.
- (57) Qiu, Y.; Odendahl, N.; Hudait, A.; Mason, R. H.; Bertram, A. K.; Paesani, F.; DeMott, P. J.; Molinero, V. Ice Nucleation Efficiency of Hydroxylated Organic Surfaces Is Controlled by Their Structural Fluctuations and Mismatch to Ice. *J. Am. Chem. Soc.* **2017**, *139*, 3052–3064.
- (58) Mochizuki, K.; Qiu, Y.; Molinero, V. Promotion of Homogeneous Ice Nucleation by Soluble Molecules. *J. Am. Chem. Soc.* **2017**, *139*, 17003–17006.

(59) Lupi, L.; Hanscam, R.; Qiu, Y.; Molinero, V. Reaction Coordinate for Ice Crystallization on a Soft Surface. *J. Phys. Chem. Lett.* **2017**, *8*, 4201–4205.